Processes Towards Sedimentation around a Reed Island in a Shallow Lake

Mariann Biró-Szilágyi[1*], Tamás Krámer[1,2], Krisztián Homoródi[1,2]

[1] Department of Hydraulic and Water Resources Engineering, Faculty of Civil Engineering, Budapest University of Technology and Economics, H-1111 Budapest, Műegyetem rakpart 3., Hungary
[2] National Laboratory for Water Science and Water Safety, Budapest University of Technology and Economics, H-1111 Budapest, Műegyetem rakpart 3., Hungary
* Corresponding author, e-mail: szilagyi.mariann@emk.bme.hu

Abstract

There are many studies on the hydromorphological impacts of emergent aquatic vegetation, but many of these focus on gravity-driven flows in riverine or tidal environments. However, an added effect of emergent vegetation in lakes is that it reduces the main external force (wind) significantly and in a spatially coherent way. We performed long Monte Carlo simulations using a 2D hydrodynamic model and a spectral wind wave model to study resuspension dynamics around a 100-m-wide reed island in southern Lake Fertő/Neusiedl. Wave-current interaction, computed in a post-processing step, was found to enhance maximum bed shear stresses only on the leeward side of the reed island, and even there to a small extent. We have found evidence that the present bed topography is close to an equilibrium where simulated combined wave-current shear stresses have a reasonably uniform exceedance probability over the critical shear stress of the bed sediment. We also found that an artificially flattened lakebed around the reed island would start evolving towards the present bed topography and grain size distribution (both of which were surveyed in the field). Despite the limitations of our modelling framework, our results illustrate the importance of how wind climate is translated to an uneven distribution of sediment entrainment around the reed island, explaining tendencies of sediment accumulation and sorting. Our results lead to a better understanding of the complicated processes involving interaction among wind, vegetation, circulation, wind waves, sediment and bathymetry.

Keywords

emergent vegetation, lake hydrodynamics, bed shear stress, simulations, field observations

1 Introduction

The physical interaction of aquatic vegetation with hydro-dynamic processes has long been investigated (e.g., [1, 2]). Emergent aquatic vegetation as an ecosystem engineer affects wind, current, surface waves and sediment motion. These plants are ecologically and structurally important because they provide habitat, take up nutrients, and contribute to shore protection in lakes and coastal regions.

In nature, emergent macrophytes occur in two forms: in extended meadows or in smaller patches [3]. The topology and density of the patches are also variable; reed tends to grow in packed islands, whereas *Schoeneplectus litoralis* forms low internal density rings [4].

In contrast to rivers or tidally influenced coastal zones, in lakes, it gains importance that emergent lake vegetation modifies the wind field compared to the open waters

(a) through the vertical structure of the atmospheric boundary layer in and above the canopy (b) and in the wake of the canopy. The recirculation zone characteristics depend on the density, height and length of the canopy. Beyond this recirculation zone, the abrupt change of roughness from reed to water (or from water to reed) gives rise to an internal boundary layer in the direction of the wind [5, 6]. An algebraic internal boundary layer (IBL) model can capture the essence of the resulting spatial inhomogeneity of wind speed and wind stress [7]. This spatial variation of the wind stress must be introduced into the hydrodynamic lake models, as simulated currents, waves, turbulent mixing and sediment motion are all affected by the accuracy of the wind stress field [7].

Several studies investigated the hydraulic effect of vegetation in unidirectional flow, mainly using laboratory experiments or numerical simulations. Laboratory experiments have typically used finite porous model patches with different densities and artificial vegetation stems to explore the flow structures inside and downstream of the patch. Zong and Nepf [8] and Sand-Jensen and Pedersen [9] studied the wake structure behind circular patches modelled as a solid body or as a porous volume. The flow separated from the top canopy edge for the solid body model. In the porous model, a less pronounced recirculation was observed, and the flow structures depended on morphological parameters: the patch diameter, stem diameter, density and emergence, as well as streamwise velocity. The turbulence intensity has two peaks at the patch wake. The first is directly behind the patch; the second is related to the generation of an oscillatory vortex street [10].

The modification of the wind field also appears in the surface wave field. The effect of individual and aggregate vegetation patches on wave dynamics was studied in and around the patches [11]. Wave damping in vegetation also depends on its morphological parameters. Wave energy (wave height) is significantly damped by vegetation drag, which can be predicted fairly well using mathematical models [12]. The sheltering effect of the vegetation (modelled as a solid obstacle) was clearly demonstrated using numerical modelling [13], acting through diffraction, refraction and the modification of local generation by wind.

Moreover, vegetation patches reduce the sediment-carrying capacity of the flow [14], trapping suspended sediment effectively within the patch. Around the patch, the flow creates both deposition and erosion zones, connected to the mean and turbulent flow fields [15]. In the wake behind a finite patch, the mean and the turbulent velocities are diminished, and the deposition of fine material is promoted [16]. It was demonstrated through hydrodynamic variables how conditions favorable to the spreading of the vegetation are created in the wake. Zong and Nepf [17] described the erosion and deposition pattern around a circular patch using different experimental conditions. On the other hand, Vandenbruwaene et al. [18] found that in the gravity-driven flows of tidal flats and rivers, velocity increases around closely packed vegetation patches, inhibiting plant growth. But these previous studies were mainly laboratory experiments or numerical studies with idealized, gravity-driven conditions or field measurements in the coastal environments.

The present research focuses on the effect of an individual reed island on water motion, bed shear stresses and the spatial distribution of bed material. In contrast to most research found in the literature that were stationary and uniform, our investigations are carried out for wind as an unsteady and multidirectional driver. The main goal of the work is to identify the hydraulic processes defining erosion and deposition patterns around a vegetation island in a field case study on Lake Fertő/Neusiedl.

Sedimentation and the lateral spreading of the reed need to accumulate over years to decades to become measurable. On this timescale, vegetation spreading is documented in aerial and satellite imagery, but the evolution of the bed shape and physical forcing was not monitored. We presume that these long-term processes can be studied using long Monte Carlo simulations, using models in which the basic processes have been validated with shorter field measurements. The simulations are driven by an unsteady wind forcing that represents the wind climate. Since detailed, long-term sediment transport modelling is difficult, it is beyond the content of the present paper. Instead, the bed shear stress from wave-current interaction is considered the proxy variable for sediment entrainment, similarly to the study of Bouma et al. [19] or D'Alpaos et al. [20]. Our goal in this paper is to identify erosion or deposition patterns in the study area through the spatial and probability distribution of the bed shear stress

2 Methods and data
Detailed data series of the hydrodynamic processes from the study site (local winds, currents and waves) were used to calibrate and validate the numerical models. It was not expected that some point field measurements will capture the long-term statistics of the hydrodynamic processes and their variability. Instead, these statistics were obtained using a Monte Carlo simulation.

2.1 Study site and field data
The case study is a reed island in Lake Fertő (also called Lake Neusiedl), a large, shallow lake stranding the Austrian-Hungarian border (Fig. 1). The dominant macrophyte is the reed (Phragmites australis), which appears in large patches and in meadows along the shoreline. The average water depth in the pelagic zone is less than 1.5 m, while the water depth in the vegetated littoral zone is up to a few decimeters and subject to great relative variation with lake volume fluctuations. The prevailing wind direction is NNW,
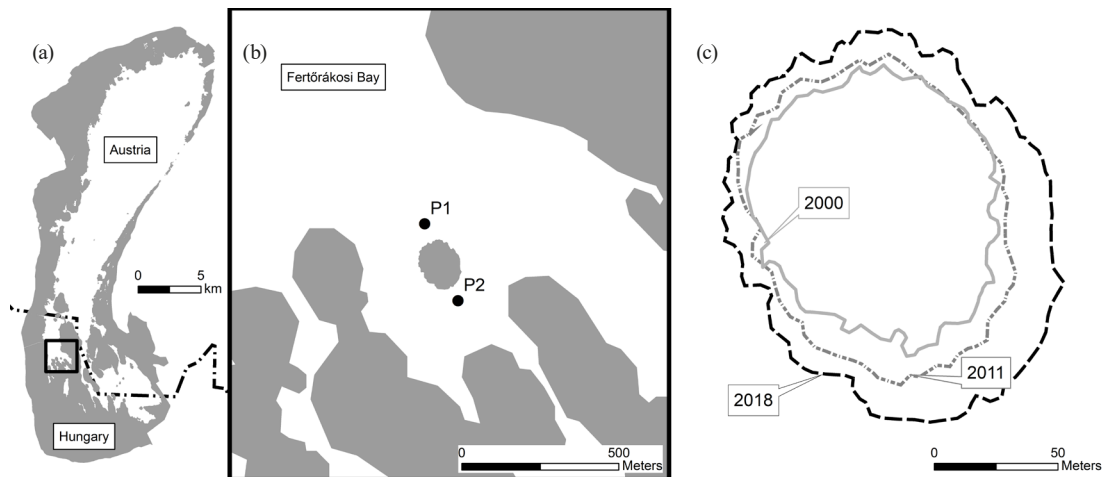
Fig. 1 Location of the study site: (a) map of Lake Fertő/Neusiedl, (b) measurement points around the reed island; (c) evolution of the extent of the island in the last 20 years
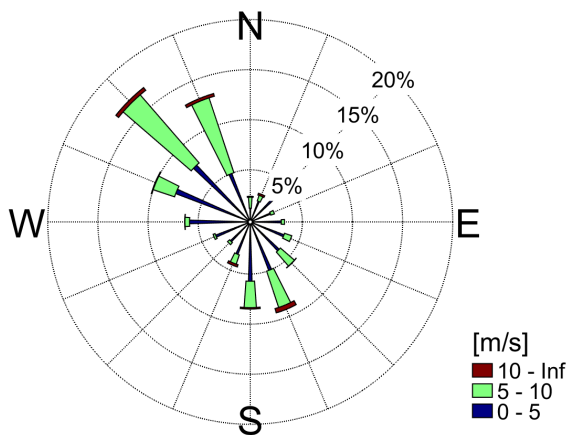

Fig. 2 Wind rose for the Fertőrákos lakeshore station for the period 25 February to 25 August 2018, with affine wind speed adjustment to match long-term statistics. Source: North-Transdanubian Water Directorate (ÉDUVIZIG)

but SSE is also frequent (Fig. 2). It must be noted that rarer wind directions can cause much higher resuspension than the prevailing ones because they increase bed shear stresses over areas that accumulate fine sediment during frequent wind events [21]. Waves are fetch-limited in Fertőrákos Bay, and their mean height depends strongly on the direction of wind.

Our investigations were carried out in the Fertőrákos Bay, around a 100-meter-diameter circular reed island that has grown noticeably over the last 20 years (Fig. 1(a)). This island is representative of the many reed patches detached from the contiguous reed belt.

Between June and August in 2018, we held a measurement campaign around the reed patch. Fig. 1(b) shows the location of the two measurement points. It also indicates the decadal evolution of the contours of the patch digitized from historical Google Earth orthophotos.

We measured wind, waves and currents at two opposite sides of the island along the prevailing wind direction: at the NNW (P1) and SSE (P2) sides (Fig. 1). Canopy properties and the bed elevation within the patch were not measured because we found that waves and currents around the island are not sensitive to the inner morphology of the island, therefore, the island could be simply modelled as a solid block obstacle.

We surveyed the bed material at 23 points around the island using an in-situ penetrometer [22]. According to penetration depths of the cones, four different sediment classes were identified: sand, sandy silt, silt and fine silt. The distribution clearly shows the asymmetry of the wave climate: mainly sand at the windward (NW) side of the study area and a mixture of finer sediment classes in the wind shadow zone (SE). Notably, fine silt was found only in the SE direction.

The grain size distribution of bed sediment near the flow measurement points P1 and P2 was determined using a laser diffraction device [23]. As expected from the penetrometer data, we found that finer grains are more abundant at point P2 than at point P1. From the median grain size diameter, we estimated the interval of critical bed shear stress for erosion using two methods, Soulsby's [24] and van Rijn's [25]. see Table 1. Bed sediment is set into motion if the combined maximum wave-current bed shear

Table 1 Main characteristics of the bed material at points P1 and P2: volume/volume share of sand (63–2000 µm), silt (2–63 µm) and clay (<63 µm) classes; median size and estimated interval of the critical bed shear stress

ID	sand	silt	clay	d_{50}	τ_{cr}
P1	29%	59%	12%	30 µm	0.07–0.088 Pa
P2	22%	58%	20%	16 µm	0.052–0.06 Pa

stress under a wave cycle, $\tau_{max,wc}$ exceeds the critical shear stress for erosion of the bed sediment, τ_{cr}, and the rate of erosion is governed by the excess $\tau_{max,wc} - \tau_{cr}$.

2.2 The numerical modeling framework

The present work is based on using a 2D hydrodynamic model (MIKE 21 FM version 2019) and a spectral wave model (SWAN version 41.31). The models are uncoupled from each other, their contribution to the bed shear stress is combined in a post-processing step. These relatively inexpensive models capture the essence of the hydrodynamics associated with morphological changes and allow long simulations. The hydrodynamic model uses the finite volume method to solve the Reynolds-averaged shallow water equations [26], thus, it is able to describe depth-averaged long waves and horizontal circulation. As to the wave model, it is a third-generation spectral wave model developed for wind-generated waves from the nearshore to the surf zone [27]. It has been applied to both deep and shallow waters [28] and was validated for Lake Fertő/Neusiedl [29].

The combined bed shear was determined in a post-processing step using the method of Soulsby and Clarke [30], which assumes that the enhancement of the wave shear stress by currents is negligible.

The model area consisted of the Fertőrákos Bay, bounded by the reed border and transects across the two northern straits that connect the bay to the rest of the lake. Wind-induced water depth fluctuations computed by the hydrodynamic model were introduced into the wave model. The flow and the wave models used the same horizontal unstructured mesh layout, with a variable mesh resolution between 10 and 100 m. The results of both models were processed at a time resolution of 10 minutes.

We assumed that the actual bed around the reed island is close to a dynamic equilibrium where erosion and deposition roughly balance each other over the timescale of a year. As a reference, we also modelled bed shear stresses over an artificially flattened bed unaffected by the reed, expecting that the modelled shear stress patterns will support the theory that the flattened bed would evolve towards the actual bathymetry. Absolute elevations in this article are given as meters above sea level (ASL), relative to the Adriatic datum of Austria used by the Austrian-Hungarian Water Commission at Lake Fertő/Neuseidl.

More specifically, two bed geometries were set up:
1. The *actual* bathymetry, as surveyed recently in 2015 in the GENESEE project [31] (Fig. 3).

2. A locally *flattened* bathymetry, where the bed elevation was lowered to a depth of 1.50 m under the mean water level of 115.50 m ASL. Beyond a distance of 160 m from the perimeter of the reed island, the bathymetry remained the *actual* one.

Water level variations due to the wind and volumetric changes are significant relative to the shallow depth of Fertőrákos Bay. In the ten years (2012–2021) leading to the currently observed morphology, the lake's mean water level varied between 115.14 m and 115.86 m ASL. Near the reed patch, wind induces a water level excursion of ± 0.05 m or more around the mean water level with a frequency of 5% [31]. To explore the effect of water level variations on the statistics, two Monte Carlo simulations were performed with the *actual* bed:
1. A 6-month simulation with a lake mean water level of 115.50 m ASL.
2. A 10-year simulation with a varying lake mean water level observed between 2012-2021. The 6-month wind was cycled periodically during this simulation.

The *flattened* bed was only simulated for the 6-month period.

The reed perimeter was treated as a closed boundary in both models. In an earlier study, we found that the effect of vegetation morphology on currents and waves is negligible, and wave attenuation is practically complete over short distances inside the reed [13]. The effect of wave reflection from the reed border was also tested. Van Gent [32]
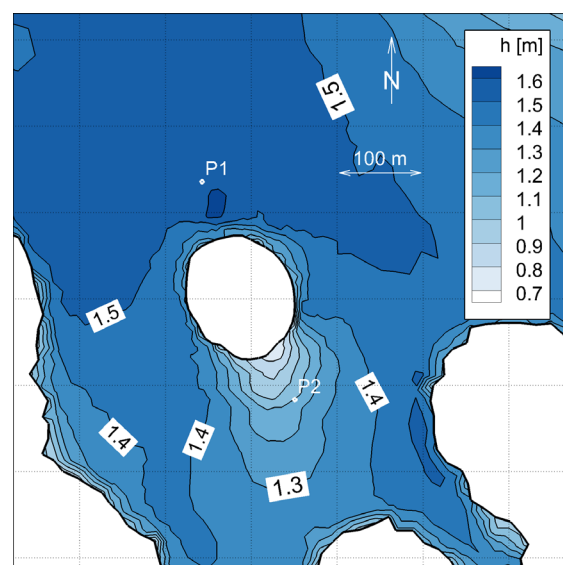

Fig. 3 The distribution of mean water depth around the reed island under a mean water level of 115.50 m above sea level

concluded that the wave energy reflection coefficient in similar cases is between 0.2-0.4. According to our numerical results using the SWAN model, within this range of the reflection coefficient, reflection has only a marginal impact on the wave field in the open lake. This is the reason why the island, as well as the rest of the reed, were blocked out from the model area, and so, only motions in the open lake were modelled.

3 Results and discussion
3.1 Time-averaged bed shear stresses
We first look at the horizontal distribution of the time-averaged bed shear stresses over the duration of the simulation (Fig. 4(a)–(c)).

The nonlinearity caused by depth fluctuations on the time-averaged $\tau_{max,wc}$ in the naturally varying lake volume simulation (Fig. 4(a) and (d)) are found to be minor. Essentially the same values are obtained with a lake volume held stationary at its mean level (Fig. 4(b) and (e)), in spite of the depth-dependence of the wind-induced lake setup in this shallow lake. This confirms that the mean statistics are well approximated with the shorter 6-month simulation at mean lake volume.

The difference between the *actual* (Fig. 4(b) and (e)) and the *flattened* bed (Fig. 4(c) and (f)) simulations with mean lake volume is striking. On the wave-exposed NW side, the *flattened* bed differs from the *actual* one only on the 50-m-wide fringe of the reed island and so, the $\tau_{max,wc}$ profiles are essentially the same. The mean shear stress gradually weakens closer to the vegetation (except for the fringe) because waves arriving from the NW quadrant are older and increase much less along the fetch than younger waves from the SE quadrant, and this difference is so pronounced that it prevails in the mean in spite of the lower frequency of SE winds.

However, the main difference between simulations with the *actual* and the *flattened* beds can be identified in the shadow zone. As the level of the *flattened* bed was set to coincide with the deepest point of the *actual* bed, it resulted in larger depths, especially in the shadow zone (marked as SE side in the profile). According to our model, the deepening caused a drop in the time-average bed shear stresses, reflecting that the attenuation of the orbital motion was stronger than the amplification of the waves in deeper water. Over the *actual* bed, time-averaged shear stress values vary in a narrow range. By contrast, over the
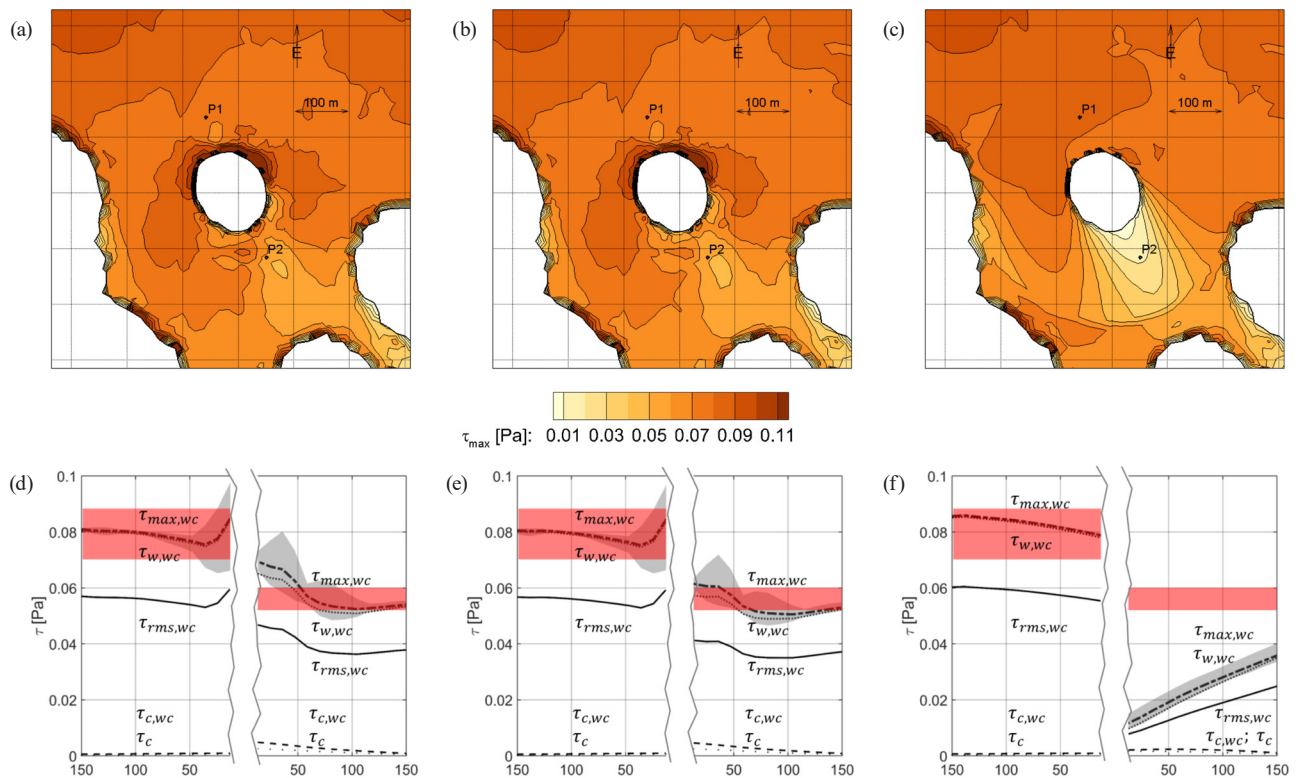
Fig. 4 (a)–(c) horizontal distribution of the time-averaged $\tau_{max,wc}$ bed shear stresses; (d)–(f) horizontal profiles of the respective upper panel along an SE oriented transect passing through P1 and P2. Red bands = range of critical bed shear stress estimated from sediment grain size. Grey bands = envelope of $\tau_{max,wc}$ contained by offsetting the transect laterally within a strip of ±25 m. (a) and (d) *actual* bed with lake volume fluctuations; (b) and (e) *actual* bed with mean lake volume; (c) and (f) *flattened* bed with mean lake volume

flattened bed, shear stresses are approximately zero at the edge of the island and increase almost linearly with fetch in the SE direction.

This impact is attributed to the sheltering from the strongest winds in the wake zone [13]. If Figs. 4(a) and (b) are compared to the water depth map in Fig. 3, the connection between time-averaged shear stresses and bathymetry becomes obvious. However, Fig. 4(c) with the *flattened* bed also reflects that wave energy penetrates laterally into the wake zone by diffraction and spreading, and waves are also locally generated. With the *actual* bed, wave refraction due to depth gradients also plays a role.

In order to simplify the visualization of various bed shear stress components, a 1D profile will be taken along the prevailing wind direction (towards SE) across the center of the reed island (Fig. 4(d)–(f)).

On average, waves dominate the bottom boundary layer. Shear stresses associated with the periodic wave motion, namely the amplitude of the oscillatory bed shear stress (τ_w), the maximum and the root-mean-square of the bed shear stress during a wave cycle under combined waves and currents ($\tau_{max,wc}$ and $\tau_{rms,wc}$, respectively) are one to two orders of magnitude higher than those associated with the current, i.e., the current-only bed shear stress (τ_c) and the wave-enhanced mean bed shear stress under a wave cycle ($\tau_{c,wc}$). Consequently, averaged over a long time, wave action dominates the compound $\tau_{max,wc}$ and $\tau_{rms,wc}$ values. The root-mean-square value $\tau_{rms,wc}$ is approximately equal to $\tau_{max,wc} / \sqrt{2}$ because currents introduce little shift in the wave orbital motion.

The red horizontal bands show the intervals of τ_{cr} already summarized in Table 1. Considering long-term averages, only $\tau_{max,wc}$ and τ_w exceed the critical bed shear stress and only at the NW side. However, time-averages do not show the whole picture.

## 3.2 Probability distribution of the bed shear stress

The time scale of the morphological response to the sheltering of a reed island is from years to decades. Even if the vegetation cover is assumed to be stationary, the lakebed will not reach a static equilibrium; it undergoes sudden erosion or deposition during extreme storms and more continuous, creeping changes due to the weaker action of frequent winds.

The net vertical sediment flux across the bottom boundary layer is governed by the excess shear stress above the critical threshold and the suspended sediment concentration above the boundary layer. The latter introduces

nonlinearity, so that the time-average shear stresses alone are insufficient to explain the morphological evolution; the probability distribution of overthreshold exceedances must also be analyzed.

We first note that the frequency of $\tau_{max,wc}$ exceeding 0.06 Pa, a representative average value of the estimated critical shear stress for erosion, is rather uniform, about 0.20–0.25 for the *actual* bed (Fig. 5). For the *flattened* bed, overthreshold exceedances are reduced markedly on the sheltered SE side of the island, a clear indication that this would be a deposition zone.

We looked further into the probability distribution functions (PDFs) of $\tau_{max,wc}$ along the NW-SE transect, at eight points, 10, 50, 100 and 150 m from the island edge on either side (see Fig. 5 for their placement). The PDFs were calculated for simulations using *original* and *flattened* bed models (Fig. 6).
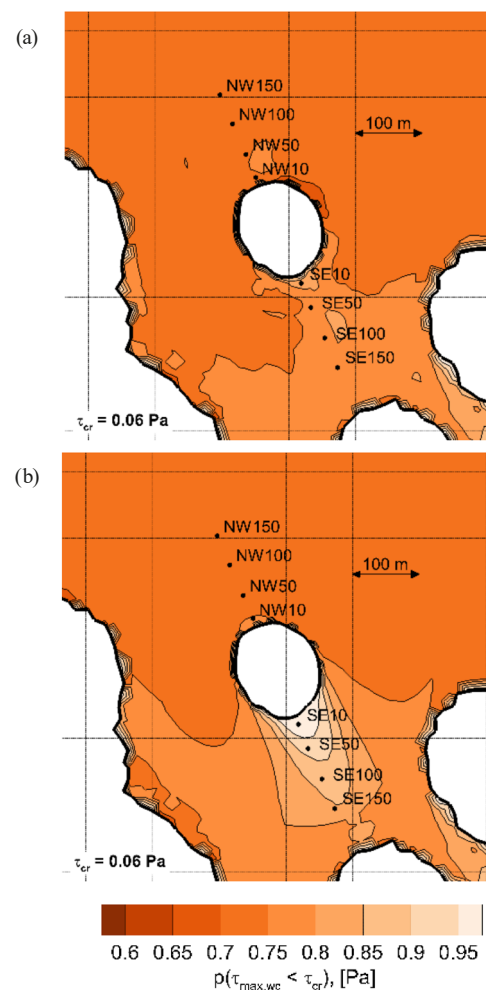
Fig. 5 Ratio of time when $\tau_{max,wc}$ was below τ_{cr} = 0.06 Pa for the actual (a) and the flattened (b) bed, based on the 6-month simulations with a stationary mean lake volume. The points labelled NW and SE show the query points for Fig. 6.
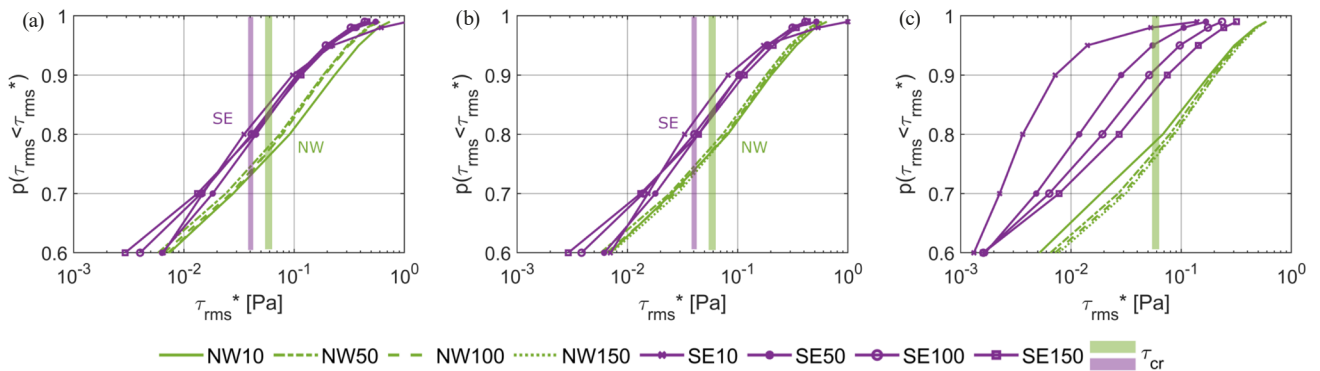
Fig. 6 Empirical probability distribution functions of $\tau_{max,wc}$, at selected points along the NW-SE centerline. Green and purple vertical bands represent the range of the critical shear stress for erosion for the NW and SE points, respectively. (a) *Actual* bed with lake volume fluctuations; (b) *actual* bed with the mean lake volume; (c) *flattened* bed with the mean lake volume

Simulations with the *actual* bed (Fig. 6(a) and (b)) revealed that the PDFs are lumped into a NW and a SE group, SE consistently having about half the maximum bed stress compared to the NW for a given probability. As already observed for the time-average values of $\tau_{max,wc}$ (Fig. 4), very similar results are obtained with the mean lake water volume than with one fluctuating around that mean. Differences are only noticeable for the two curves at 10 m distance from the reed island, leading to a small decrease of the maximum bed shear stress if lake volume variations are considered. The respective critical shear stress for erosion (lower for the NW points) is exceeded about 25% of the time, implying that the bed and its grain size distribution have almost reached a steady state.

From a morphological point of view, the *flattened* bed can be considered an undisturbed starting point (Fig. 6(c)), when the bed hasn't adapted yet to the reed island. The lowest $\tau_{max,wc}$ values appear at 10 m distance from the reed edge in the sheltered zone (SE10), where the bed shear stress exceeds the critical value only 5% of the time, whereas that frequency is between 25–30% in the case of the NW side. Here, the relevant τ_{cr} on both the NW and SE sides is that of the finer grain composition indicated with the purple vertical band because the bed material is assumed to be uniform before the disturbance by the reed island is introduced. Thus, it has been clearly demonstrated that the more sheltered side of the reed island is a deposition zone. In line with the contours seen in Fig. 5(b)), overthreshold exceedances become gradually more frequent with distance on the sheltered SE side.

Interestingly, an analysis shows that the wave-current bottom boundary layer is in the rough turbulent regime 90% of the time, according to the criterion of the Soulsby and Clarke method [30]. It is dominated by wave-induced

stress about half of the time and the other half purely by currents. Waves respond much faster to changes of wind than currents do: they die off within 10 minutes after a strong wind has abated. In contrast, horizontal circulation and seiche need hours to attenuate in Lake Fertő/Neusiedl. That explains why wind-induced currents of considerable magnitude occur so often alongside short, low-amplitude waves that are unable to set the bottom boundary layer into a periodic motion.

3.3 Relation between bed shear stress, depth and bed material

It is notable that the bed material is consistently coarser on the wave-sheltered side of the island (Fig. 7(b)), closely in line with the spatial distribution of the bed shear stresses (Fig. 5(a)).

The scatter plot between the time-averaged water depth and $\tau_{max,wc}$ indicate a slightly positive trend in the case of the actual bathymetry (Fig. 7(a)). Higher $\tau_{max,wc}$ values are paired with sandy bed material and water depths exceeding 1.4 m, whereas lower values come with an abundance of silt and a water depth between 1.0 and 1.4 m. We remark that points with $\tau_{max,wc} > 1$ Pa come from the southern edge of the model domain where the solution is more variable, so they do not reflect the effect of the reed island. Therefore, we find a strong link between the shear stresses and bed morphology.

In case of the *flattened* bed (not plotted), a uniform bed composition would not result in an equilibrium with the highly uneven shear stresses already shown in Fig. 5(b). At the short horizontal spatial scale of the reed patch, currents are easily capable to transport suspended sediment from wave-exposed to the wave-sheltered zones, leading to an effective horizontal mixing. Consistent bed shear
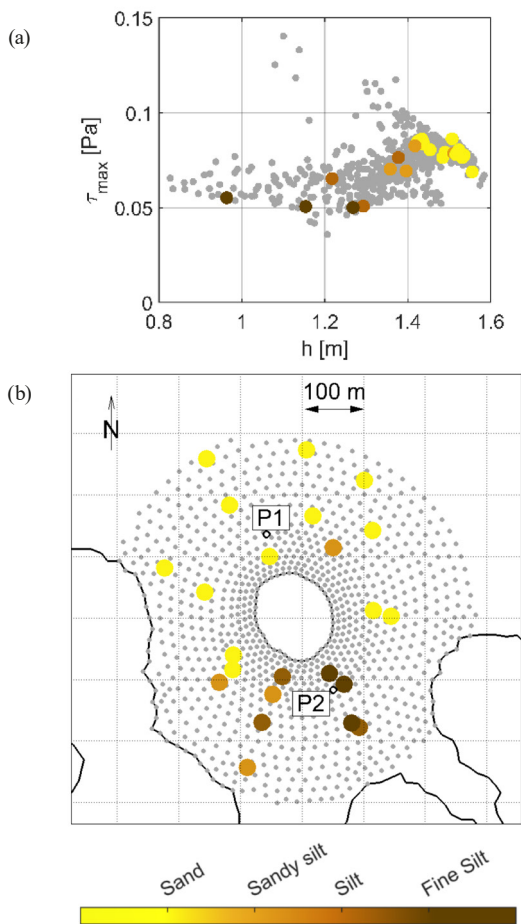
Fig. 7 (a) Scatter plot of the time-averaged $\tau_{max,wc}$ v. water depth at the computational points in a 200 m diameter circle around the reed island for the *actual* bed, based on the simulations with the mean lake volume. (b) Horizontal layout of the computational points. Points where the bed material was surveyed are enlarged and colored according to the given scale

stress gradients will therefore result in bed material sorting and leeward deposition, slowly leading towards the *actual* bed morphology.

4 Conclusions

A 2D hydrodynamic model was used in conjunction with a spectral wind wave model to study resuspension dynamics around a 100 m diameter reed island in southern Lake Fertő/Neusiedl. Nonlinear wave-current interaction was included in a post-processing step. Wave-current interaction was found to enhance maximum bed shear stresses only a little, and most considerably on the leeward side of the reed island. The horizontal distribution of the bed sediment composition was mapped during a field survey.

The models successfully predicted events recorded in the field at two observation points, on the wave-exposed and on the wave-sheltered side of the island. A Monte

Carlo analysis was performed using a 10-year simulation (approximated using interpolation between a discrete set of simulations with different stationary lake volume). Interestingly, in spite of the substantial amplitude of wind surface setup with respect to water depth, very similar bottom shear stress statistics could be obtained using a 6-month simulation in which the lake volume was kept stationary at its 10-year average value. This is a useful result to optimize the computational demand of further probabilistic numerical analyses.

We have found evidence that the present bed topography is close to an equilibrium where simulated combined wave-current shear stresses have a reasonably uniform exceedance probability over the critical shear stress of the bed sediment. An artificially flattened lakebed around the reed island would start evolving towards the present bed topography and grain size distribution. We have not explored how long this evolution would take, as that would call for a sediment transport model and much longer simulations.

What makes the hydraulic impact of emergent vegetation in lakes different from gravity-induced riverine or tidal environments is that vegetation reduces the main forcing component, wind, significantly and in a spatially coherent way. Since the studied reed patch is far from the longitudinal seiche node, lake oscillation generates weak currents and circulatory currents prevail. If the reed island were located close to the node, then stress induced by oscillatory currents would be stronger and possibly induce scouring around the perimeter of the island, as Vandenbruwaene [18] and Bouma [19] have found for vegetation patches on tidal flats.

Although the modeling framework used in the present study has proven effective, it does have some limitations. Bed shear stress is only a proxy variable for bed change tendencies. For a more accurate study, a suspended sediment transport and a vegetation model should be integrated into the framework, preferably coupled with the wind wave and hydrodynamic models to provide feedback via bed changes and reed progression. More field data on the critical bed shear stresses and sediment concentration under various conditions need to be collected.

Despite the simple assumptions and the limitations of our modelling framework, it illustrates the importance of how wind climate is translated to an uneven distribution of sediment entrainment around the reed island, explaining tendencies of sediment accumulation and sorting. Our results lead to a better understanding of the complicated processes involving the interaction among wind,

vegetation, circulation, wind waves, sediment and bathymetry, therefore, the framework developed here presents a useful tool for further studies in Lake Fertő/Neusiedl.

References

[1] Nepf, H. M. "Drag, turbulence, and diffusion in flow through emergent vegetation", Water Resources Research, 35(2), pp. 479–489, 1999.
https://doi.org/10.1029/1998WR900069

[2] Folkard, A. M. "Hydrodynamics of model Posidonia oceanica patches in shallow water", Limnology and Oceanography, 50(5), pp. 1592–1600, 2005.
https://doi.org/10.4319/lo.2005.50.5.1592

[3] Schoelynck, J., Creëlle, S., Buis, K., De Mulder, T., Emsens, W.-J., …, Folkard, A. "What is a macrophyte patch? Patch identification in aquatic ecosystems and guidelines for consistent delineation", Ecohydrology & Hydrobiology, 18(1), pp. 1–9, 2018.
https://doi.org/10.1016/j.ecohyd.2017.10.005

[4] Szőke, E., Brolly, G., Takács G., Kalicz, P. "Sudden spreading of club-rush (Schoenoplectus litoralis) in Lake Neusiedl", In: Proceedings of the Hydrocarpath International Conference Catchment Processes in Regional Hydrology: Experiments, Patterns and Predictions, Vienna, Austria, 2017, pp. 1–7. ISBN 978-963-359-092-8

[5] Markfort, C. D., Porté-Agel, F., Stefan, H. G. "Canopy-wake dynamics and wind sheltering effects on Earth surface fluxes", Environmental Fluid Mechanics, 14(3), pp. 663–697, 2013.
https://doi.org/10.1007/s10652-013-9313-4

[6] Kiss, M., Józsa, J. "Wind profile and shear stress at reed-open water interface – Recent research achievements in Lake Fertő", Pollack Periodica, 10(2), pp. 107–122, 2015.
https://doi.org/10.1556/606.2015.10.2.10

[7] Józsa, J., Milici, B., Napoli, E. "Numerical simulation of internal boundary-layer development and comparison with atmospheric data", Boundary-Layer Meteorology, 123, pp. 159–175, 2007.
https://doi.org/10.1007/s10546-006-9134-9

[8] Zong, L., Nepf, H. "Vortex development behind a finite porous obstruction in a channel", Journal of Fluid Mechanics, 691, pp. 368–391, 2012.
https://doi.org/10.1017/jfm.2011.479

[9] Sand-Jensen, K., Pedersen, M. L. "Streamlining of plant patches in streams", Freshwater Biology, 53(4), pp. 714–726, 2008.
https://doi.org/10.1111/j.1365-2427.2007.01928.x

[10] Chen, Z., Ortiz, A., Zong, L., Nepf, H. "The wake structure behind a porous obstruction and its implications for deposition near a finite patch of emergent vegetation", Water Resources Research, 48(9), W09517, 2012.
https://doi.org/10.1029/2012WR012224

[11] Maza, M., Lara, J. L., Losada, I. J. "Solitary wave attenuation by vegetation patches", Advances in Water Resources, 98, pp. 159–172, 2016.
https://doi.org/10.1016/j.advwatres.2016.10.021

[12] Lövstedt, C. B., Larson, M. "Wave damping in reed: Field measurements and mathematical modeling", Journal of Hydraulic Engineering, 136(4), pp. 222–233, 2010.
https://doi.org/10.1061/(ASCE)HY.1943-7900.0000167

[13] Szilágyi, M., Homoródi, K., Krámer, T. "Investigation of wave dynamics around a vegetation patch in a shallow lake", In: Water Research and Innovations in Digital Era, Riga Technical University, Riga, Latvia, 2021, pp. 244–251. ISBN 978-9934-22-618-2.

[14] Le Bouteiller, C., Venditti, J. G. "Vegetation-driven morphodynamic adjustments of a sand bed", Geophysical Research Letters, 41(11), pp. 3876–3883, 2014.
https://doi.org/10.1002/2014GL060155

[15] Follett, E. M., Nepf, H. M. "Sediment patterns near a model patch of reedy emergent vegetation", Geomorphology, 179, pp. 141–151, 2012.
https://doi.org/10.1016/j.geomorph.2012.08.006

[16] Liu, C., Nepf, H. "Sediment deposition within and around a finite patch of model vegetation over a range of channel velocity", Water Resources Research, 52(1), pp. 600–612, 2016.
https://doi.org/10.1002/2015WR018249

[17] Zong, L., Nepf, H. "Vortex development behind a finite porous obstruction in a channel", Journal of Fluid Mechanics, 691, pp. 368–391, 2012.
https://doi.org/10.1017/jfm.2011.479

[18] Vandenbruwaene, W., Temmerman, S., Bouma, T. J., Klaassen, P. C., de Vries, M. B., …, Meire, P. "Flow interaction with dynamic vegetation patches: Implications for biogeomorphic evolution of a tidal landscape", Journal of Geophysical Research-Earth, 116(F1), F01008, 2011.
https://doi.org/10.1029/2010JF001788

[19] Bouma, T. J., van Duren, L. A., Temmerman, S., Claverie, T., Blanco-Garcia, A., Ysebaert, T., Herman, P. M. J. "Spatial flow and sedimentation patterns within patches of epibenthic structures: Combining field, flume and modelling experiments", Continental Shelf Research, 27(8), pp. 1020–1045, 2007.
https://doi.org/10.1016/j.csr.2005.12.019

[20] D'Alpaos, A., Carniello, L., Rinaldo, A. "Statistical mechanics of wind wave-induced erosion in shallow tidal basins: Inferences from the Venice Lagoon", Geophysical Research Letters, 40(13), pp. 3402–3407, 2013.
https://doi.org/10.1002/grl.50666

[21] Lövstedt, C. B., Bengtsson, L. "The role of non-prevailing wind direction on resuspension and redistribution of sediments in a shallow lake", Aquatic Sciences, 70(3), pp. 304–313, 2008.
https://doi.org/10.1007/S00027-008-8047-8

[22] Håkanson, L., Jansson, M. "Principles of Lake Sedimentology", Springer-Verlag, 1983. ISBN 3-540-12645-7

[23] Sequoia Scientific, Inc. "LISST-PORTABLE│XR Manual Version 1.3", [pdf] Sequoia Scientific, Inc., Bellevue, WA, 2018. Available at: https://www.sequoiasci.com/wp-content/uploads/2015/06/LISST-PortableXR-Manual-Version-1_3.pdf [Accessed: 31 March 2023]

[24] Soulsby, R. "Dynamics of Marine Sands", Thomas Telford, 1998. ISBN 978-0727725844

[25] van Rijn, L. C. "Unified view of sediment transport by currents and waves. I: Initiation of motion, bed roughness, and bed-load transport", Journal of Hydraulic Engineering, 133(6), pp. 649–667, 2007.
https://doi.org/10.1061/(asce)0733-9429(2007)133:6(649)

[26] DHI "MIKE 21 and MIKE 3 Flow Model FM, Hydrodynamic and transport module", Hørsholm, Denmark, 2017. [online] Available at: https://manuals.mikepoweredbydhi.help/2017/Coast_and_Sea/MIKE_321_FM_Scientific_Doc.pdf [Accessed: 31. 03. 2023]

[27] Booij, N., Ris, R. C., Holthuijsen, L. H. "A third-generation wave model for coastal regions: 1. Model description and validation", Journal of Geophysical Research: Oceans, 104(C4), pp. 7649–7666, 1999.
https://doi.org/10.1029/98JC02622

[28] Mao, M., van der Westhuysen, A. J., Xia, M., Schwab, D. J., Chawla, A. "Modeling wind waves from deep to shallow waters in Lake Michigan using unstructured SWAN", Journal of Geophysical Research: Oceans, 121(6), pp. 3836–3865, 2016.
https://doi.org/10.1002/2015JC011340

[29] Homoródi, K., Józsa, J., Krámer, T. "On the 2D modelling aspects of wind-induced waves in shallow, fetch-limited lakes", Periodica Polytechnica, Civil Engineering, 56(2), pp. 127–140, 2012.
https://doi.org/10.3311/PP.CI.2012-2.01

[30] Soulsby, R. L., Clarke, S. "Bed shear-stresses under combined waves and currents on smooth and rough beds", HR Wallingford, Rep. TR 137, 2005. [online] Available at: https://eprints.hrwallingford.com/558/1/TR137.pdf [Accessed: 31. 03. 2023]

[31] Krámer, T., Szilágyi, J. and Nagy, E. "Investigations supporting water management planning to protect the water quality of Lake Neusiedl. Hydrological and hydrodynamic conditions", Research report, Interreg project AT-HU 53, ÉDUVIZIG, Győr, 2019.

[32] van Gent, M. R. A. "ODIFLORA - Vegetative wave damping as bank protection", TU Delft, Technical report, 1994.
https://doi.org/10.13140/RG.2.1.3296.5363